

Wigner Crystallization in a Quasi-3D Electronic System

B.A. Piot¹, Z. Jiang^{2,3}, C.R. Dean¹, L.W. Engel², G. Gervais¹, L.N. Pfeiffer⁴ and K.W. West⁴

¹*Department of Physics, McGill University, Montreal, H3A 2T8, CANADA*

²*National High Magnetic Field Laboratory, Tallahassee, Florida 32310, USA*

³*Department of Physics, Columbia University, New York, New York 10027, USA*

⁴*Bell Labs, Alcatel-Lucent Incorporation, Murray Hill, New Jersey 07974, USA and*

Nature Physics 4, 936 - 939 (2008) Published online: 5 October 2008
<http://www.nature.com/nphys/journal/v4/n12/abs/nphys1094.html>

PACS numbers: 73.40.Lp, 73.43.Qt

When a strong magnetic field is applied perpendicularly (along z) to a sheet confining electrons to two dimensions (x - y), highly correlated states emerge as a result of the interplay between electron-electron interactions, confinement and disorder. These so-called fractional quantum Hall (FQH) liquids [1] form a series of states which ultimately give way to a periodic electron solid that crystallizes at high magnetic fields. This quantum phase of electrons has been identified previously as a disorder-pinned two-dimensional Wigner crystal with broken translational symmetry in the x - y plane [2, 3, 4, 5, 6, 7, 8]. Here, we report our discovery of a new insulating quantum phase of electrons when a very high magnetic field, up to 45T, is applied in a geometry *parallel* (y -direction) to the two-dimensional electron sheet. Our data point towards this new quantum phase being an electron solid in a ‘quasi-3D’ configuration induced by orbital coupling with the parallel field.

The formation of an electron solid has been observed previously at very high magnetic fields where less than $\frac{1}{5}$ of the lowest Landau level describing the orbital dynamics is occupied by electrons, or at zero magnetic field in extremely dilute 2D systems realized on helium surfaces [9]. Recently, a 1D Wigner crystal was also reported for electrons in carbon nanotubes [10]. Here, we present evidences for another possibility where the crystallization would occur in a ‘quasi-3D’ electronic system, evolving continuously from a disorder-pinned 2D state. In our work, a two-dimensional electron gas (2DEG) is rotated inside a magnetic field by a tilting angle θ , so that an in-plane magnetic field B_{\parallel} is added parallel to the 2DEG. Provided this field be large enough, it has been proposed theoretically [11] that the electron solid energy would become lower than that of the FQH liquid at Landau level filling factors $\nu = n_s/(eB_{\perp}/h)$, where n_s is the electron density, significantly higher than for the conventional 2D Wigner crystal in which $\nu \lesssim \frac{1}{5}$. A tilt-induced liquid-to-insulator transition has been observed in a 2D hole system [12, 13, 14] in which the insulating phase, ini-

tially located at $\nu \lesssim \frac{1}{3}$, was shifted close to $\nu = \frac{2}{3}$ with increasing θ . However, such a tilt-induced transition for electrons has so far been elusive. Here, combining a relatively ‘thick’ high-mobility 2DEG and very high parallel magnetic fields B_{\parallel} to enhance orbital coupling, we report a transition from a FQH liquid to an insulating phase in an *electron* system.

In Fig. 1, we report in a 3D plot the longitudinal resistance, R_{xx} of sample C as a function of the perpendicular magnetic field for different tilting angles. In the perpendicular configuration, *i.e.* when $\theta=0^{\circ}$, we observe the usual FQH series characterized by a vanishing longitudinal resistance due to the opening of a many-body gap in the density of states. At higher perpendicular magnetic fields, for filling factors lower than $\nu = \frac{1}{5}$, a divergence of R_{xx} corresponding to the onset of a deep insulating state ($R_{xx} \gtrsim 800k\Omega$), previously identified as a disorder-pinned Wigner Crystal, is observed [6, 7, 8]. A reentrance of the insulating state ($R_{xx} \sim 400k\Omega$) is also observed in a narrow region between $\nu = \frac{1}{5}$ and $\nu = \frac{2}{9}$ [15]. As the tilting angle is further increased, the onset of the divergence shifts to lower perpendicular fields, signaling the appearance of an insulating phase at higher filling factors, and approaching $\nu = \frac{2}{3}$ at $\theta = 68.35^{\circ}$. The temperature dependence of R_{xx} at $\theta = 68.35^{\circ}$ and $B_{\perp}=10.7$ T is shown in the inset. At this magnetic field, R_{xx} increases exponentially with $1/T$, as observed in the zero tilt insulating phase below $\nu = \frac{1}{5}$ [15, 16], thus confirming the similarity of this new quantum phase with the 2D Wigner crystal phase at zero tilt. At this angle, we also observed a critical field $B_{\perp,c}$ separating a metallic ($\partial R_{xx}/\partial T > 0$) from an insulating region ($\partial R_{xx}/\partial T < 0$) for which R_{xx} does not depend on temperature, characteristic of a metal-to-insulator transition[17]. We also observe FQH states (such as at $\nu = 1/3$) that remain robust for intermediate angles even though the neighbouring (higher) filling factor region becomes insulating, *i.e.* showing up as resistance peaks in Fig. 1. This is reminiscent of the re-entrant insulating phase observed in the pure perpendicular field case.

To further investigate the nature of this new insulating quantum phase, we have measured the FQH gap at

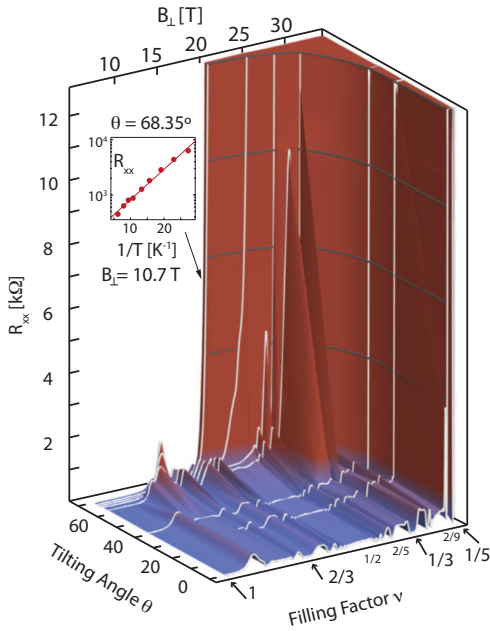


FIG. 1: Longitudinal resistance R_{xx} versus tilt and filling factor ν . The resistance of sample C is shown as a function of the perpendicular magnetic field B_{\perp} (or equivalently the filling factor ν) for different tilting angles θ and $T \simeq 35$ mK. White lines are actual data, and the trend in between is extrapolated as a guide-to-the-eye. The resistance value is emphasized by a colourmap, with the black lines corresponding to equi-resistance. Inset: temperature dependence of R_{xx} at $\theta=68.35^{\circ}$ and $B_{\perp}=10.7$ T.

$\nu = \frac{1}{3}, \frac{2}{5}$ as a function of the tilting angle θ . In Fig. 2 the longitudinal resistance R_{xx} of sample A at $\nu = \frac{1}{3}$ is plotted on a semi-log scale as a function of the inverse temperature $1/T$, for various tilting angles. R_{xx} clearly follows a thermally activated behaviour where $R_{xx} \propto e^{-\frac{\Delta}{2k_B T}}$ over a few decades, allowing us to extract the thermally activated gap, Δ . The resulting values are reported in Fig. 3a as a function of the total magnetic field, B_{total} . At high tilting angles (total magnetic field), both the $\frac{1}{3}$ and $\frac{2}{5}$ gaps are reduced. For the $\frac{1}{3}$ FQH state, the weakening of the gaps *cannot* be accounted for by spin effects since its ground state is fully spin-polarized. Similarly, at the large B_{\perp} involved here, the $\nu = \frac{2}{5}$ FQH state is most likely spin-polarised [18, 19], so no spin-related effects are expected to reduce the gap. In addition, pure disorder-related effects occurring at high θ [20] cannot account for the gap reduction observed here. The calculation of R_{xx} at 41.96° with disorder-induced gap suppression owing to an increase in Landau level broadening [21] (dashed line in Fig. 2) does not qualitatively agree with the observed linear trend. The Landau level broadening used to fit the onset of the R_{xx} decrease is seven times larger than measured from the Shubnikov de Haas oscillations at zero tilt. This is inconsistent with the observation of well-developed FQH states at this angle, $\theta = 41.96^{\circ}$.

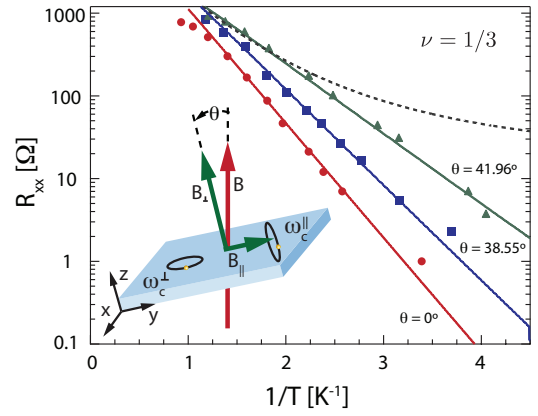


FIG. 2: Thermal activation plots at $\nu = 1/3$ for sample A. The longitudinal resistance R_{xx} is plotted as a function of $1/T$ for different tilting angles θ (solid symbols, error bars smaller than symbols). The solid lines are fit enabling the extraction of the thermally activated FQH gaps. Calculation of R_{xx} for (pure) disorder-induced gap suppression at 41.96° is shown with a dashed line (see text).

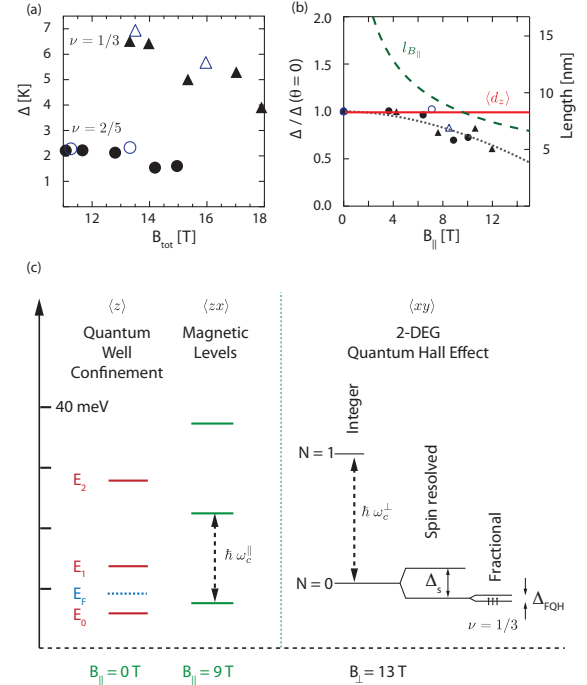


FIG. 3: Activation energy gaps and relevant energy scales. (a) Thermally activated gap at $\nu = 1/3$ (triangles) and $\nu = 2/5$ (circles) as a function of the total magnetic field B_{total} . Sample A (closed symbols) and B (open symbols). (b) Thermally activated gap normalized with respect to their $\theta = 0^{\circ}$ value, at $\nu = 1/3$ (triangles) and $\nu = 2/5$ (circles) as a function of the parallel magnetic field B_{\parallel} . The dotted line is a guide to the eye. Magnetic length $l_{B_{\parallel}}$ associated with B_{\parallel} (dashed line) and average thickness of the 2DEG in the z direction $\langle d_z \rangle$ (solid line) (right scale). All data error bars smaller than symbols. (c) Energy diagram (see text). All energies are calculated with respect to the bottom of the conduction band (dashed horizontal line) and are shown to scale.

In Fig. 3b we plot the same thermally activated gap normalized by their value at $\theta = 0^\circ$, as a function of the parallel magnetic field B_{\parallel} . Interestingly, a similar collapse of the FQH states is obtained as a function of B_{\parallel} . More strikingly, the gap reduction begins at $B_{\parallel} \sim 7\text{T}$ which is very close to the parallel magnetic field $B_{\parallel} \sim 9\text{T}$ where the magnetic length $l_{B_{\parallel}} = \sqrt{\hbar/eB_{\parallel}} = 8.5\text{ nm}$ associated with B_{\parallel} approaches the average thickness of the 2DEG in the \mathbf{z} direction, $\langle d_z \rangle = 8.3\text{ nm}$ (calculated using Ref.[22]). This is strong evidence for the collapse of the FQH gaps to be directly related to orbital coupling with the parallel field, becoming stronger when electrons are confined to dimensions smaller than the initial 2DEG thickness. For $B_{\parallel} \gtrsim 10\text{T}$, the electron gas now defines a ‘quasi-3D’ system, with the quantum well now primarily providing a sample with a finite width in the \mathbf{z} direction.

One can obtain an estimate for the angle $\theta_{c_{1/3}}$ for which the $\nu = \frac{1}{3}$ gap vanishes completely by extrapolating the B_{\parallel} trend observed in Fig. 3b. The resulting angle, $\theta_{c_{1/3}}^{ap} \sim 58 \pm 5^\circ$, correlates very well with the angle at which the insulating phase appears at $\nu = \frac{1}{3}$, estimated from Fig. 1 to be $\theta_{c_{1/3}}^{R_{xx}} \sim 61. \pm 2^\circ$. This reinforces our interpretation for the collapse of the FQH gap at $\nu = \frac{1}{3}$, and the related emergence of an insulating phase to be driven by orbital coupling to the parallel field.

It is instructive to consider all relevant energies as tilt is increased, and these are depicted schematically in Fig. 3c. In the \mathbf{x} - \mathbf{y} plane, the conventional quantum Hall effects and associated Landau levels are separated by the cyclotron energy $\hbar\omega_c^\perp = \hbar eB_\perp/m^*$, represented here for the perpendicular magnetic field where the $\nu = \frac{1}{3}$ FQH state is observed in sample A, $B_\perp \sim 13\text{ T}$. The spin gap, Δ_s , is shown for the $N = 0$ Landau level, and Δ_{FQH} gives the magnitude of the $\nu = \frac{1}{3}$ FQH gap. Along the confinement axis \mathbf{z} , we use calculations for the confinement energy of a 40 nm wide quantum well as given in Ref.[23], and report here the first three electric subbands, E_0 , E_1 and E_2 . The Fermi energy E_F is indicated in absence of a magnetic field, showing that all electrons are confined in the first subband, E_0 . When a sufficient parallel magnetic field is applied, magnetic levels take over the confinement levels in determining the \mathbf{z} energy; these ‘Landau-like’ levels are separated by the ‘parallel cyclotron energy’ $\hbar\omega_c^\parallel$ and they determine the energy in the \mathbf{z} - \mathbf{x} plane [24]. When the parallel magnetic field is further increased, the occupation of the lowest ‘Landau-like’ magnetic level with a degeneracy eB_{\parallel}/h is reduced. We note, however, that we described for simplicity two independent sub-systems in the \mathbf{x} - \mathbf{y} and \mathbf{z} - \mathbf{x} planes, whereas in reality they are naturally coupled in the \mathbf{x} direction.

From the data in Fig. 1, we can construct a phase diagram for the ‘quasi-3D’ insulator at high tilt (parallel field). For this, we (arbitrarily) define a critical filling factor ν_{c_1} corresponding to the smallest ν value for which a FQH state is observed, as well as a critical filling factor

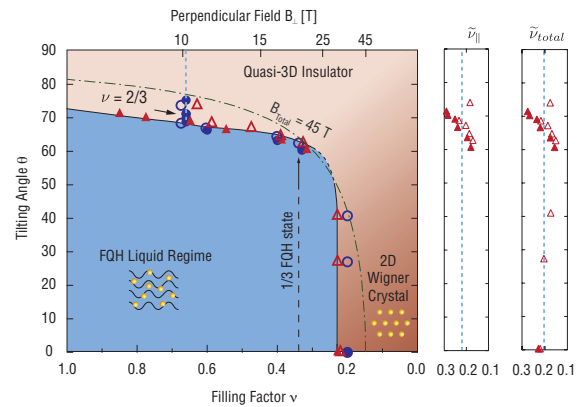


FIG. 4: Phase diagram for the ‘quasi-3D’ insulator at $T \simeq 35\text{mK}$. Critical filling factors ν_{c_1} (circles) and ν_{c_2} (triangles) (defined in text) as a function of the tilting angle θ . The open symbols are data extracted from Fig. 1, and the closed symbols were obtained on a separate cooldown. The $B_{total}=45\text{ T}$ line (dash-dot) determines the experimental observable range. Right panel: ‘parallel (total) filling factor’ $\tilde{\nu}_{\parallel}$ ($\tilde{\nu}_{total}$) (defined in the text) associated with the critical filling factor ν_{c_2} (triangles). The vertical dashed line is the average value of $\tilde{\nu}_{\parallel}$ ($\tilde{\nu}_{total}$).

tor ν_{c_2} corresponding to the largest ν value for which the resistance value exceeds $h/2e^2=12.91\text{ k}\Omega$. One can therefore view ν_{c_1} as the liquid phase termination, and ν_{c_2} as the onset of the insulating phase. The criterion for ν_{c_2} is justified by the inset of Fig.1 which shows the sample to be already insulating for this resistance value. In this context, the reentrance of the insulating phase, usually observed between the $\nu = \frac{2}{9}$ and $\nu = \frac{1}{5}$, is characterized by $\nu_{c_2} > \nu_{c_1}$. These critical filling factors ν_{c_1} (circles) and ν_{c_2} (triangles) are plotted in Fig. 4 as a function of the tilting angle θ , and at base temperature $T \simeq 35\text{ mK}$, with closed and open symbols denoting data obtained during two separate cooldowns. As the tilt angle θ is increased, a higher total magnetic field is required to achieve the perpendicular field necessary to observe the $\nu = \frac{1}{5}$ FQH state and the neighbouring insulating region. This restricts our tilting range for that state to angles $\theta \lesssim 42^\circ$, within the 45T of our magnet indicated as a dash-dotted line. However, further tilt of the sample shifts the insulating phase to higher filling factors, so that it reappears within our field range at angles $\theta \gtrsim 60^\circ$. The persistence of the $\nu = \frac{2}{3}$ FQH state at $\theta \gtrsim 70^\circ$ results in having a reentrant phase ($\nu_{c_2} > \nu_{c_1}$) in this region of the phase diagram.

The smooth crossover between the low- θ and high- θ regions of the phase diagram is evidence for a continuous distortion of the perpendicular-field dominated 2D Wigner crystal to an electron solid stabilized in a ‘quasi-3D’ geometry. The steep divergence of R_{xx} preceding the ‘quasi-3D’ insulator, as well as the existence of reentrant states, are analogous to what is observed for the 2D Wigner crystal in the perpendicular configuration.

Recent numerical calculations [11] have predicted the ground state energy of the solid phase to be very close to the liquid under sufficient tilting angles, *e.g.* $\theta \gtrsim 45^\circ$ at $\nu = \frac{1}{3}$. For strong parallel fields, Landau-like magnetic levels in the \mathbf{z} - \mathbf{x} plane should be forming as the 2DEG becomes a ‘quasi-3D’ system. The non-zero perpendicular field B_\perp is nevertheless absolutely required here to prevent the electronic system from being free along the \mathbf{y} direction and the Landau quantization to be smeared out by the free kinetic energy. At high tilt angles, B_\perp thus provides an effective magnetic confinement in the \mathbf{y} -direction so as to recreate a pseudo-2D system along \mathbf{z} - \mathbf{x} . In this regime, $\theta \gtrsim 60^\circ$, we can define a *parallel* filling factor associated with the parallel field component, $\tilde{\nu}_\parallel = n_s/(eB_\parallel/h)$ describing the occupation in the first \mathbf{z} - \mathbf{x} magnetic level. Here, we have assumed n_s to remain unmodified by the field axis. The right panel of Fig. 4 shows a scatter plot for the values obtained for $\tilde{\nu}_\parallel$ at the onset of the insulating phase ν_{c_2} and $\theta \gtrsim 60^\circ$, where $l_{B_\parallel} \lesssim 6$ nm. The transitions from a FQH liquid to an insulating phase in this regime occur at an average parallel filling factor $\langle \tilde{\nu}_\parallel \rangle = 0.22$, shown by a dashed vertical line. We also define a *total* filling factor $\tilde{\nu}_{total} \equiv n_s/(eB_{total}/h)$, equal to $\tilde{\nu}_\parallel$ (ν) in the high B_\parallel (B_\perp) limit. Using this definition, the transitions observed here occur close to $\frac{1}{5}$ over the whole θ range, $\theta = [0, 70^\circ]$ (right panel in Fig. 4). The values of $\tilde{\nu}_{total}$ at the transitions are similar to those associated with the onset of the conventional 2D \mathbf{x} - \mathbf{y} Wigner crystal, at $\nu < \frac{1}{5}$, therefore suggesting a possible stabilization of an electron solid by the *total* magnetic field due to a reduction of the occupation of the quantized orbital energy level. A continuous evolution of the liquid-insulator transitions can be seen in the main panel of Fig. 4, where the phase boundary clearly mimics that of the total field. The solid phase would occur for l_{B_\parallel} sufficiently small relative to the quantum well width, so that electrons may acquire the freedom to minimize their mutual repulsion by adjusting their positions in the \mathbf{z} -direction. We note, however, that the exact structure of this electron solid cannot at present be conjectured and remains an open question which will be better addressed by microwave experiments probing the pinning modes of the crystal.

This work has been supported by the Natural Sciences and Engineering Research Council of Canada (NSERC), the Canada Fund for Innovation (CFI), the Canadian Institute for Advanced Research (CIFAR), FQRNT (Québec), the Alfred P. Sloan Foundation (G.G.), and the NSF under DMR-03-52738 (Z.J.). We thank H.L. Stormer and D.C. Tsui for helpful discussions, and J. Hedberg, G. Jones, T. Murphy and E. Palm for technical assistance. A portion of this work was performed at the National High Magnetic Field Laboratory, which is supported by NSF Cooperative Agreement No. DMR-0084173, by the State of Florida, and by the DOE.

-
- [1] D. C. Tsui, H. L. Stormer, and A. C. Gossard, *Two-dimensional magnetotransport in the extreme quantum limit*, Phys. Rev. Lett. **48**, 1559-1562 (1982).
 - [2] E. Wigner, *On the interaction of electrons in metals*, Phys. Rev. **46**, 1002-1011 (1934).
 - [3] Y. E. Lozovik and V. I. Yudson, *Crystallization of a two-dimensional electron gas in a magnetic field*, JETP Lett. **22**, 11-12 (1975).
 - [4] P. K. Lam and S. M. Girvin, *Liquid-solid transition and the fractional quantum-Hall effect*, Phys. Rev. B **30**, 473-475 (1984).
 - [5] D. Levesque, J. J. Weis, and A. H. MacDonald, *Crystallization of the incompressible quantum-fluid state of a two-dimensional electron gas in a strong magnetic field*, Phys. Rev. B **30**, 1056-1058 (1984).
 - [6] F. I. B. Williams, P. A. Wright, R. G. Clark, E. Y. Andrei, G. Deville, D. C. Glatzli, O. Probst, B. Etienne, C. Dorin, C. T. Foxon, and J. J. Harris, *Conduction threshold and pinning frequency of magnetically induced Wigner solid*, Phys. Rev. Lett. **66**, 3285-3288 (1991).
 - [7] Y. P. Chen, G. Sambandamurthy, Z. H. Wang, R. M. Lewis, L. W. Engel, D. C. Tsui, P. D. Ye, L. N. Pfeiffer, and K. W. West, *Melting of a 2D quantum electron solid in high magnetic field*, Nature Phys. **2**, 452-455 (2006).
 - [8] See for a review M. Shayegan, in *Perspectives in Quantum Hall Effects*, edited by S. Das Sarma and A. Pinczuk (Wiley, New York, 1997), Chap. 9.
 - [9] C. C. Grimes and G. Adams, *Evidence for a liquid-to-crystal phase transition in a classical, two-dimensional sheet of electrons*, Phys. Rev. Lett. **42**, 795-798 (1979).
 - [10] V. V. Deshpande and M Bockrath, *The one-dimensional Wigner crystal in carbon nanotubes*, Nature Phys. **4**, 314-318 (2008).
 - [11] Y. Yu and S. Yang, *Effect of the tilted field in fractional quantum Hall systems: numerical studies for the solid-liquid transition*, Phys. Rev. B **66**, 245318 (2002).
 - [12] W. Pan, G. A. Csáthy, D. C. Tsui, L. N. Pfeiffer, and K. W. West, *Transition from a fractional quantum Hall liquid to an electron solid at Landau level filling $\nu = 1/3$ in tilted magnetic fields*, Phys. Rev. B **71**, 035302 (2005).
 - [13] M. B. Santos, Y. W. Suen, M. Shayegan, Y. P. Li, L. W. Engel, and D. C. Tsui, *Observation of a reentrant insulating phase near the $1/3$ fractional quantum Hall liquid in a two-dimensional hole system*, Phys. Rev. Lett. **68**, 1188-1191 (1992).
 - [14] G. A. Csáthy, H. Noh, D. C. Tsui, L. N. Pfeiffer, and K. W. West, *Magnetic-Field-induced insulating phases at large r_s* , Phys. Rev. Lett. **94**, 226802 (2005).
 - [15] H. W. Jiang, R. L. Willett, H. L. Stormer, D. C. Tsui, L. N. Pfeiffer, and K. W. West, *Quantum liquid versus electron solid around $\nu = 1/5$ Landau-level filling*, Phys. Rev. Lett. **65**, 633-636 (1990).
 - [16] R. L. Willett, H. L. Stormer, D. C. Tsui, L. N. Pfeiffer, K. W. West, and K. W. Baldwin, *Termination of the series of fractional quantum hall states at small filling factors*, Phys. Rev. B **38**, 7881-7884 (1988).
 - [17] D. Shahar, D.C. Tsui, M. Shayegan, R.N. Bhatt, and J.E. Cunningham, *Universal conductivity at the quantum Hall liquid to insulator transition*, Phys. Rev. Lett. **74**, 4511-4514 (1995).
 - [18] D. R. Leadley, R. J. Nicholas, D. K. Maude, A. N. Utjuzh,

- J. C. Portal, J. J. Harris, and C. T. Foxon, *Fractional quantum Hall effect measurements at zero g factor*, Phys. Rev. Lett. **79**, 4246-4249 (1997).
- [19] W. Kang, J.B. Young, S.T. Hannahs, E. Palm, K.L. Campman, and A.C. Gossard, *Evidence for a spin transition in the $\nu=2/5$ fractional quantum Hall effect*, Phys. Rev. B. **56**, 12776-12779 (1997).
- [20] S. Das Sarma and E. H. Hwang, *Parallel magnetic field induced giant magnetoresistance in low density quasi-two-dimensional layers*, Phys. Rev. Lett. **84**, 5596-5599 (2000).
- [21] A. Usher, R. J. Nicholas, J. J. Harris, and C. T. Foxon, *Observation of magnetic excitons and spin waves in activation studies of a two-dimensional electron gas*, Phys. Rev. B **41**, 1129-1134 (1990).
- [22] M. P. Stopa and S. Das Sarma, *Density scaling and optical properties of semiconductor parabolic and square quantum wells*, Phys. Rev. B **45**, 8526-8534 (1992).
- [23] F. Stern and J. N. Schulman, *Superlattices and Microstructures Calculated effects of interface grading in GaAs-Ga_{1-x}Al_xAs quantum wells*, **1**, 303-305 (1985).
- [24] M. P. Stopa and S. Das Sarma, *Parabolic-quantum-well self-consistent electronic structure in a longitudinal magnetic field: subband depopulation*, Phys. Rev. B **40**, 10048-10051 (1989).

Methods

The 2DEGs studied here are 40 nm wide modulation-doped GaAs quantum wells, all from the same wafer grown by molecular beam epitaxy. They are referred to as samples A, B and C, and have densities $n_s=1.05, 1.06$ and $1.52 \times 10^{11} \text{ cm}^{-2}$ and corresponding mobilities $\mu=12(2), 8(2)$ and $14(2) \times 10^6 \text{ cm}^2/\text{V}\cdot\text{s}$, respectively. The samples were cooled in a dilution fridge with base temperature $T \simeq 35 \text{ mK}$ installed inside a hybrid superconducting/resistive magnet capable of reaching a total magnetic field of 45T. Treatment with a red LED was used during the cooldown. Transport measurements were performed using a standard low-frequency lock-in technique at low excitation current, $I_{exc} \sim 2 - 100 \text{ nA}$. The sample was tilted with respect to the total magnetic field B_{total} (see lower left cartoon in Fig. 2) using an in-situ rotation stage. The tilting angle θ was determined from the shift of the resistance minimum of well-known integer quantum Hall states, according to $B_{\perp} = B_{total} \cdot \cos(\theta)$.